Microphase Separation of Linear and Cyclic Block Copolymers Poly(styrene-*b*-isoprene): SAXS Experiments

S. Lecommandoux,[†] R. Borsali,[*,†] M. Schappacher,[†] A. Deffieux,[†] T. Narayanan,[‡] and C. Rochas[§]

Laboratoire de Chimie des Polymères Organiques, CNRS, ENSCPB-Bordeaux-1 University, 16 Avenue Pey Berland 33607 PESSAC, France, ESRF, Grenoble, France, and Laboratoire de Spectrométrie Physique, Université J. Fourier Grenoble 1, 38402 St Martin d'Hères, France

Received October 29, 2003; Revised Manuscript Received December 2, 2003

ABSTRACT: We have studied the effect of cyclization of a linear poly(styrene-*b*-isoprene) PS-*b*-PI copolymer system on the morphology of the organized nanostructures. The linear and the cyclic copolymers have exactly the same degree of polymerization, i.e., 290 for PS and 110 for PI, corresponding to a volume fraction $\Phi_{PS} = 0.78$. We used small-angle X-rays scattering to characterize the microphase separation and to highlight the difference in the microstructure between linear (several scattering peaks) and cyclic copolymer systems (single scattering peak). Our results show that the linear PS−PI is microphase-separated and organized in a 2-d hexagonal packing (reflections 1:$\sqrt{3}$:$\sqrt{4}$:$\sqrt{7}$:$\sqrt{9}$:$\sqrt{12}$: etc.) as expected at this volume fraction. In contrast, the morphology adopted by cyclic copolymer chains is a liquidlike micellar phase (single scattering peak). Both the domain spacing as well as the temperature effects were found very sensitive to the cyclization of the linear diblock copolymer. This results shows that the cyclization of a linear block copolymer induces remarkable changes in the morphology of the organized nanostructure.

I. Introduction

Block copolymer systems, including diblock A−B or triblock A−B−A, constitute a very important class of polymers that lead to fascinating organizations or self-assemblies in both solution and bulk states. They can form micelles[1,2] when the solvent is bad for one block and good for the other. They can also form a broad panel of microstructures/organized morphologies[3,4] (lamellae, hexagonal cylinders, cubic arrays of spheres, gyroid, etc.) on length scales of 10−100 nm in particular when cast from solutions (in good solvent for both blocks A and B). The morphologies (shape and size) of the micelles as well as the bulk organized structures in the ordered phases depend strongly on the total degree of polymerization ($N = N_A + N_B$), the Flory−Huggins χ_{AB} parameter that quantifies the incompatibility between the blocks, and the volume fraction of the A-block. It is worth recalling here that the microphase separation or the self-assembly in block copolymer systems are the consequences of unfavorable enthalpy and of a small entropy of mixing.

The phase diagram of linear coil−coil diblock copolymers has been extensively studied and is well established.[5,6] Recently a lot of work was done on the self-assembly of rod−coil diblock copolymers.[7] This is far the case of block copolymers having different architectures such as the following: (i) both blocks are rigid to form the so-called once-broken rod diblock copolymer or (ii) both blocks are flexible and linked to form ring diblock copolymers. However, the last case where the extremities of the two blocks are flexible and linked to form a ring diblock copolymer has already been studied theoretically.[8−10] These models predicted a transition from the disordered to an ordered phase (microphase separation) at (χN, $q_m R_{gt}$) = (17.8, 2.88) for a 50/50 diblock copolymer as compared to the classical result for linear diblocks for which (χN, $q_m R_{gt}$) = (10.5, 1.95).

Experimental confirmations require the preparation of linear and cyclic diblocks with same composition. From a synthesis point of view, it involves to covalently link the two functional end groups of a linear copolymer in order to form a copolymer ring. Three main strategies have been developed for that purpose. One is based on the bimolecular end-to-end ring closure of a living anionic *A−B−A* triblock precursor by a bifunctional nucleophilic compound.[11,12] The second strategy consists of the unimolecular coupling of a *A−B* diblock linear precursor in the presence of a catalyst.[13] A third method by monomer insertion into cyclic initiator by a radical mechanism has been used to develop block copolymers based on acrylate and acrylamide monomers.[14] The first two approaches yield to cyclic diblock A_2−B or A−B which can be compared respectively to their corresponding A_2−B or A−B linear diblock of same composition and degree of polymerization. As far the disordered state is concerned, we have carried out recently small-angle neutron scattering (SANS) on linear and cyclic PSd-PSh and PSd-PI in a mixture of *d*-toluene and *h*-toluene satisfying the zero average contrast (ZAC) conditions. The results show the existence of a scattering peak for the cyclic copolymer case whose position q^* is shifted to high q values as compared to the linear block copolymer in good agreement with the earlier theoretical predictions.[15] In addition, studies in micellar state have been performed in our group[16] on linear and cyclic PS−PI and by Hadjichristidis et al. on cyclic polystyrene-*b*-polybutadiene (PS-*b*-PB) and their PS-*b*-PB-*b*-PS triblock precursors.[12]

In those studies,[16] we have shown that the micelles obtained—in different solvents (heptane, decane, etc., bad solvent for the PS)—from linear PS-*b*-PI are spheri-

* Corresponding author: E-mail: borsali@enscpb.fr.
† ENSCPB-Bordeaux-1 University.
‡ ESRF.
§ Université J. Fourier Grenoble 1.

10.1021/ma035627r CCC: $27.50
Published on Web 02/13/2004

Scheme 1. Schematic Representation of a Linear and Cyclic Diblock Copolymer.

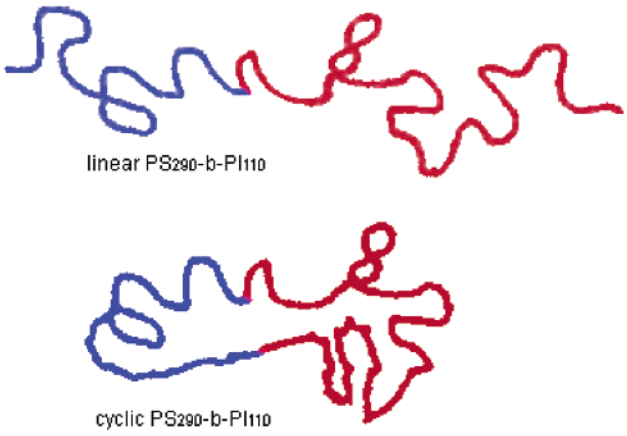

cal (50 nm in diameter) whereas those arising from cyclic PS-*b*-PI can have several thermodynamically stable morphologies such as planar "sunflower", spheres, "Y-junctions" and giant wormlike micelles whose length are concentration dependent and can be as long as 1 μm. Eventually, at higher concentrations, cyclic copolymer chains self-assembled into vesicles. These results were highlighted using static and dynamic light scattering (SLS, DLS), SAXS under shear, TEM and in situ freeze-drying Cryo-TEM, and AFM experiments.

More recently, experimental studies on films using SAXS and TEM made of cyclic polystyrene-*b*-polybutadiene (PS-*b*-PB) and their PS-*b*-PB-*b*-PS triblock precursors and made of cyclic PS-*b*-PI and their PS-*b*-PI-*b*-PS triblock precursors were reported respectively by Hadjichristidis et al.[17] and Takano et al.[18] In these works it was concluded that the architectural difference leads to differences essentially in domain spacing: the cyclic morphology always has smaller domain spacing as compared to its corresponding linear triblock. It was also found that connecting the end blocks of a triblock to form a cyclic block increases the tendency for the interface to curve away from the connected end blocks.[17]

In the present paper, we compare the scattering properties—namely in the ordered phases (microphase separation)—using SAXS of cyclic diblock copolymer PS-*b*-PI with their corresponding linear diblock PS-*b*-PI having exactly the same molar mass and volume fraction. The same linear PS-*b*-PI has been connected to form cyclic block copolymer. In this study, we would like to address and to try to answer the question of the topological constraints in cyclic block copolymers on the phase diagram as compared to simple linear diblocks. Linear AB diblock copolymers do not present any constraint in terms of loops in either of the two A and B domain spacing while AB cyclic diblock copolymers, combine a "looped" in both domains whose junctions are at the interface, thus investigating the effect of a "double constraint" on the microphase separation (Scheme 1). As it will be shown and discussed within this work, this "double constraint" induces remarkable and sensitive changes in the morphologies of microstructures obtained from linear and from cyclic copolymer chains.

Cyclic block copolymers are expected to have smaller domain spacing than their corresponding linear copolymers: this has been discussed by Marko[9] and us[8] in 1993. The microphase separation of cyclic and linear diblock copolymers having the same composition (volume fraction 50%) and molar mass leads to microphase separation with lamellar spacing ratio of a cyclic to its corresponding diblock copolymer of about $[(qR)^*_{lin}/(qR_g)^*_{Cycl}] = 0.67$ in the weak segregation limit using random phase approximation (RPA)[8] or Monte Carlo simulations.[10] This value was recalculated by Thomas et al.[11c] and was found to be almost independent of N ranging from 0.6 to 0.62 for diblock copolymers in the lamellar microstructure.

Table 1. Characteristics of the Copolymers Used in This Work

copolymer	DP_{PS} [a]	DP_{PI} [b]	M_w [c] (10^3 g/mol)
linearPS_{290}-*b*-PI_{110}	290	110	37
cyclicPS_{290}-*b*-PI_{110}	290	110	37

[a] From SEC molar mass of PS blocks using PS standards. [b] From NMR analysis of the diblock copolymer and molar mass of PS. [c] From MALS−SEC analysis.

II. Experimental Section

II-1. Synthesis. The cyclic polystyrene-*b*-isoprene (PS-*b*-PI) was prepared by direct coupling of α-isopropylidene-1,1-dihydroxymethyl-ω-diethylacetal heterodifunctional polystyrene-*b*-isoprene linear copolymer under highly diluted conditions and in the presence of an acid catalyst. This method of synthesis permits to have exactly the same degree of polymerization (DP) for each PS and PI block for linear and cyclic copolymers.[13]

As shown in Table 1, the average degree of polymerization of the polyisoprene block is roughly $^1/_3$ of the DP for the polystyrene block for both the linear and cyclic copolymers. The linear and the cyclic copolymers have exactly the same degree of polymerization, i.e., 290 for PS and 110 for PI, corresponding to a volume fraction $\Phi_{PS} = 0.78$ and a polydispersity index less than 1.1.

II-2. Sample Preparation. First, 1 mm thick films made from block copolymer chains were cast from 10 wt % solutions in toluene (a good solvent for both PS and PI) containing 0.1 w% of Irganox as an antioxidant. The evaporation of solvent was carried out slowly at room temperature for 2 weeks and then in a vacuum oven at room temperature for 2 days. Finally, the samples were heated to about 20 °C above the transition temperature of the PS block in order to anneal the films for 1 day under vacuum, and then the temperature was allowed to slowly come back to room temperature. With such a method of sample preparation (annealing process above the T_g of both blocks), we are confident that our samples are in the equilibrium state. One notes, however, that previous studies by Hashimoto et al.[19] have shown that solvent casting PS-*b*-PI copolymers from toluene can result in nonequilibrium domain sizes.

II-3. Morphological Characterization. Small-angle X-ray scattering (SAXS) was used to identify the types of structures and domain spacing in nano-organized films made from linear and cyclic diblocks. Preliminary measurements at room temperature were performed at the high brilliance beamlines (ID2 and BM2) of the European Synchrotron Radiation Facility (ESRF), in Grenoble, France. The beam size was 0.3 mm × 0.3 mm. The incident X-ray wavelength (λ) and the sample-to-detector distance were 1 Å and 10 m for ID2 and 0.775 Å and 1.5 m for BM2. SAXS patterns were recorded using an image intensified CCD detector. Most of the experiments carried out at different temperatures were performed using Cu K radiation (1.54 Å wavelength) using a Nanostar from Bruker AXS (operating at 40 kV, 35 mA). A CCD detector (Siemens Hi-Star), at a sample/detector distance of 106.2 cm, was used to record scattering patterns.

III. Results and Discussion

III-1. General Trends. Figure 1 illustrates the azimuthal averaged scattering intensities measured in films of both systems at room temperature. The insert

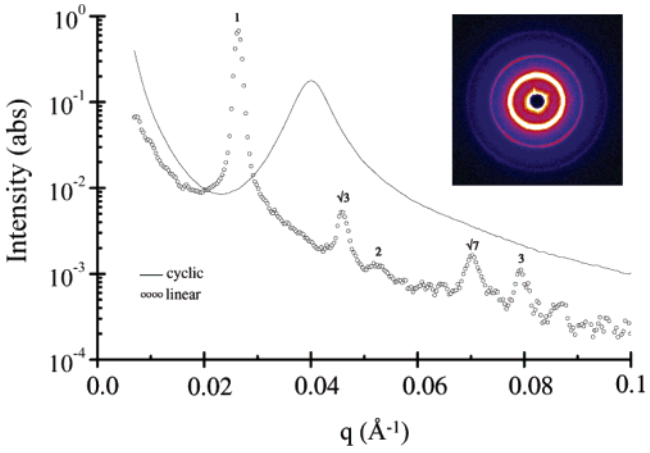

Figure 1. SAXS intensity profiles of linear and cyclic PS_{290}-*b*-PI_{110} obtained at room temperature (synchrotron, ESRF).

diagram displays the 2d-dectector image obtained from the linear block copolymer nanostructured film. The observed profiles reveal clearly different scattering behaviors. The SAXS results for linear copolymer indicate that the structure resembles a hexagonally packed cylindrical microdomains, as judged from the positions of higher order scattering maximum, appearing at the scattering vectors q of 1, $\sqrt{3}$, $\sqrt{4}$, $\sqrt{7}$, and $\sqrt{9}$. Considering the composition of the diblock copolymer (i.e., the volume fraction $\Phi_{PS} = 0.78$), one can conclude that the exact structure corresponds to hexagonal cylinders of PI in a matrix of PS with an interccolumnar distance of $d = 260$Å (for cylindrical domains: $d = 4\pi/\sqrt{3}q$). In contrast, the SAXS results corresponding to the cyclic case having exactly the same composition is completely different. First, only one very broad and diffuse scattering peak can be observed, traducing a poor organization of the system at large scale. One sees that the height of the scattered intensity for cyclic copolymers remains comparatively smaller than that of the linear case. Moreover, the wave vector position of the scattering peak is shifted to higher q values ($q_{cyc}^* = 0.040$ Å^{-1}) indicating a shorter scale of the microstructure as compared to the linear one ($q_{lin}^* = 0.028$ Å^{-1}).

These results (heights and peaks position) are in good agreement with the RPA model regarding the scattering profiles near the ordered/disordered phase transition for linear and cyclic block copolymers systems.[9,10] Indeed, comparing the size of the equivalent radius of gyration of linear and cyclic diblock copolymers (illustrated in Scheme 1) based on mean field calculations, gives a ratio (q_{lin}^*/q_{Cycl}^*) = 0.67. Experimentally, the ratio of the scattering position of linear over cyclic gives q_l/q_c = 0.028/0.040 = 0.7, thus confirming the RPA mean field theoretical approach and the cyclic architecture of the block copolymer chain (namely that the $R_{g\ linear}$ is $\sqrt{2}$ $R_{g\ cyclic}$). As only one broad scattering peak has been observed for cyclic block copolymer PS_{290}-*b*-PI_{110}, the exact structure of the microphase separation is difficult to assign. At this stage, one can conclude that the cyclic PS_{290}-*b*-PI_{110} maybe in the disordered state as compared to the 2d hexagonal ordered morphology observed for the equivalent linear. To go further on the analysis, one can calculate the χN values that characterize the transition from the disordered to an ordered phase for linear $(\chi N)_{lin}$ and cyclic $(\chi N)_{cyc}$, using the following relation to calculate the Flory−Huggins parameter χ:[20]

$$(\chi_{PS-PI}) = -0.0522 + 48.8/T\ (\mathrm{K}) \qquad (1)$$

It is assumed in this case that the Flory−Huggins parameter χ_{PS-PI} is the same for linear and cyclic block copolymer chains. Using the total number of repeated units $N = 400$ for linear and cyclic diblocks, we thus obtained for room temperature ($\chi_{PS-PI} = 0.1116$) a value of this parameter $(\chi N)_{lin} = (\chi N)_{cyc} = 44.6$ which is much higher than the critical value calculated for the disordered to ordered state ($\chi N \approx 22$ for linear and $\chi N \approx 35$ at the composition $\Phi_{PS} = 0.78$).[5,10] On the basis of these values of χN and on the scattering profiles, it is very clear that at room temperature the linear block copolymer system is in its ordered phase. On the other hand and although the scattering curve shows only one broad peak the value of χN allows us to conclude that the cyclic PS_{290}-*b*-PI_{110} is in its ordered state with however a fairly low ordering of polyisoprene spheres in a matrix of polystyrene, as commonly observed for low ordered cubic structures. Such an hypothetical "ordering", although very low, is based on other observations of liquidlike micellar phase that was found using SAXS to be stable in asymmetric PS-*b*-PI diblock copolymers by Schwab et al.[21] Rheological measurements also confirmed that diblock or even triblock copolymers with $\Phi < 0.2$ (for either block) exhibit a "liquidlike" viscoelastic response corresponding to this liquid spherical micelle phase.[22] In other words, the linear system is microphase separated in a 2d-cylindrical phase (existence of several scattering peaks and the χN value is higher than the critical one). This is obviously not very clear for the cyclic case (single broad scattering peak), although the χN value is above the critical one but has been calculated assuming the same value of χ in both systems. To gain a better understanding on the organized structures in both systems, one possibility is to examine the effects of temperature near the ordered-disordered transition.

III-2. Temperature Effect and Determination of the Order—Disorder Transition Temperature (ODT). The temperature dependence of SAXS profiles are illustrated in Figure 2, parts a and b, respectively, for linear and cyclic PS_{290}-*b*-PI_{110}. There are different ways, based on mean field theory, of analyzing SAXS profiles to investigate the ODT of block copolymers. For instance, one can use the plot of (i) the reciprocal of the maximum scattered intensity (I_m^{-1}) vs the reciprocal of absolute temperature (T^{-1}) or (ii) the wavelength of a dominant mode of fluctuation concentration ($D = 2\pi/q_{max}$) vs T^{-1}. According to Leibler's model[5] that is based on the Landau-type mean field approach, I_m^{-1} is expected to decrease linearly vs T^{-1} in the disordered state, meaning that

$$I_m^{-1} \propto a - b/T \qquad (2)$$

where a and b are positive constants. This assumes that the temperature dependence of the Flory−Huggins interaction parameter χ_{A-B} is given by

$$\chi_{A-B} = A + B/T \qquad (3)$$

where A and B are constants. In that model,[5] it is predicted that the domain spacing D (or q_m) in the disordered state is independent of the temperature, except for a small temperature variation which originates from the dependence of the radius of gyration $R_g(T)$ of the whole block copolymer chain, generally a stretching of the chain.

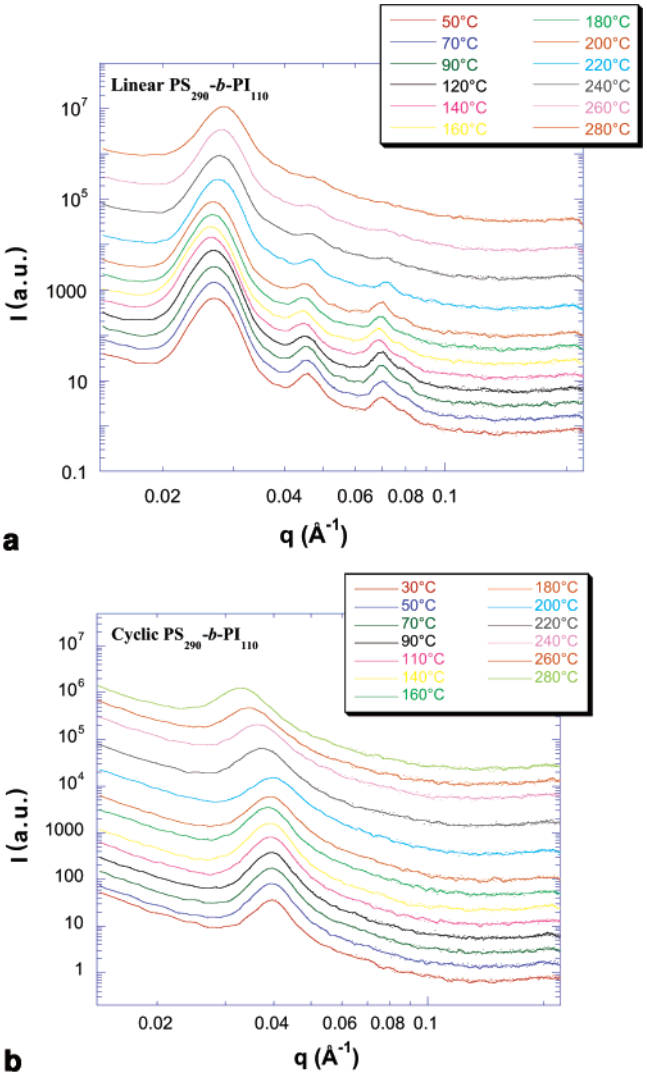

Figure 2. SAXS intensity profiles as a function of temperature obtained for (a) linear and (b) cyclic PS_{290}-*b*-PI_{110}. The data are shifted vertically for each temperature for clarity.

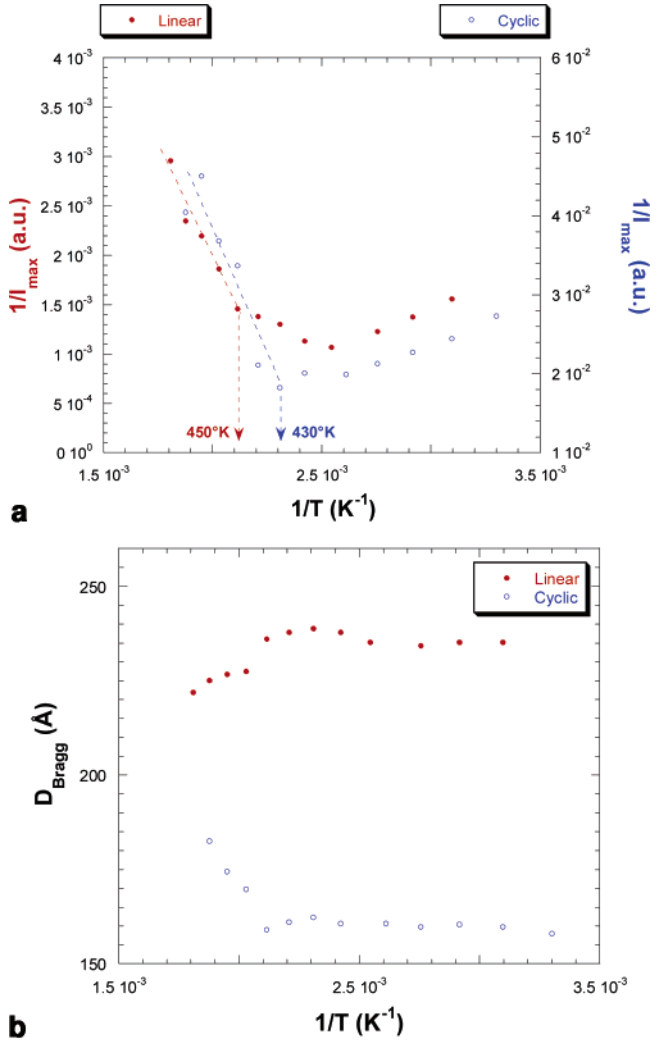

Figure 3. Plots of (a) I_m^{-1} vs T^{-1} and (b) D vs T^{-1} for linear and cyclic PS_{290}-*b*-PI_{110}.

Figure 3 represents the plots of I_m^{-1} vs T^{-1} (Figure 3a) and D vs T^{-1} (Figure 3b) for linear and cyclic PS_{290}-*b*-PI_{110}. Figure 3a shows a linear decrease in I_m^{-1} for both systems in the disordered state and almost constant values in the low temperature range (ordered state), as theoretically predicted. The crossover (discontinuity) of I_m^{-1} vs T^{-1} allows us to determine the ODTs: these are 450 and 430 K, respectively, for linear and cyclic block copolymers. As previously observed by Rosedal et al.,[23] the use of the divergence of I_m^{-1} vs T^{-1} from a straight line to determine the ODT can lead to an overestimated value. We have tried in our case to determine the ODT from q_m^{-1} and/or peak width vs T^{-1}. The precision of the data did not allowed a perfect agreement between the methods for the determination of the ODT. Interestingly, it is possible that the crossover could result from the transition from the disordered, linear mean-field region to the disordered, non-mean-field region due to concentration fluctuations instead of the disordered-to-ordered transition. To overcome this ODT determination, on can also carry out experiments using dynamic mechanical analysis or static birefringence which are currently under progress. From eq 1, one can thus calculate the critical $(\chi N)_{ODT}$ value corresponding to the experimentally measured ODT. These data are summarized in Table 2. For linear diblock copolymer PS_{290}-*b*-PI_{110}, the critical $(\chi N)_{ODT}$ value is 22.5, thus in very good agreement with theoretical predictions ($\chi N \approx 22$).[5] Consequently, the linear system is organized in a 2d-cyclindrical morphology and all the features for such organization are captured in the experimental evidence. As far as the cyclic PS_{290}-*b*-PI_{110} is concerned, the experimental critical value of $(\chi N)_{ODT}$ determined from the ODT is 24.5. This value is however very different from the theoretical prediction ($\chi N \approx 35$).[10] At this stage, on may explain this discrepancy on the basis of the following arguments. The first explanation might be related to the model itself that over-estimated the increase in compatibility between the block in the cyclic case as compared to the linear: there is a breakdown of the balance between unfavorable enthalpy and entropy of mixing when the block copolymer chain is cyclic. A second explanation could be attributed to $(\chi N)_{ODT}$ value that has been deduced for the cyclic diblock assuming the same relation of the evolution of χ[20] with temperature for linear ones. This approximation was somehow tempting to use since no relation exists in the literature of the effect of cyclization on the evolution of the χ parameter. Indeed, such a hypothesis might be questionable as one can anticipate that due to the entropic constraints in cyclics, the evolution of the interaction parameter with the tem-

Table 2. Structure, Domain Spacings, and Thermal Stability for Linear and Cyclic PS_{290}-*b*-PI_{110}

copolymer PS_{290}-*b*-PI_{110}	structure	q_{max} ($Å^{-1}$)[a]	D_{Bragg} (Å)[b]	$D_{spacing}$ (Å)[c]	T_{ODT} (K)	$(\chi N)_{ODT}$	$(\chi N)_{theor}$
linear	cylinder	0.028	224	259	450	22.5	22[d]
cyclic	sphere	0.040	157	192	430	24.5	35[e]

[a] Scattering vector at the first peak position in the SAXS profile. [b] Bragg conditions: $D_{Bragg} = 2\pi/q_{max}$. [c] Domain spacing which is function of the geometry: for cylinders $D_{spacing} = \sqrt{(4/3)}2\pi/q_{max}$, for spheres $D_{spacing} = \sqrt{(3/2)}2\pi/q_{max}$. [d] Value obtained from ref 5. [e] Value obtained from ref 10.

perature should be different from the linear diblocks. We believe that this second explanation can be at the origin of this discrepancy and we are currently working on the development of an expression of this χ parameter with the temperature for cyclic diblocks.

As for the data and particularly the variation of I_m^{-1} vs T^{-1} (Figure 3a) and the breakdown of this behavior obtained here for cyclic diblock copolymer confirm that an ordered structure is present at low temperature, even if only a broad peak was observed. These observations thus corroborate a low organization of spheres in a liquid spherical micelle morphology as suggested before. If this phase were a cubic structure we estimate the inter-sphere distance $d = 192$ Å ($2\sqrt{3}\pi/\sqrt{2}q$).

Interestingly, in Figure 3b, the variation of D vs T^{-1} for linear and cyclic PS_{290}-*b*-PI_{110} shows an original behavior for cyclic copolymers. Indeed, the generally observed behavior is an almost independent evolution of the domain spacing D below the ODT, which is confirmed here for both cases. This is a consequence of a stretching of the polymer chains when approaching the ODT. Here the linear PS_{290}-*b*-PI_{110} respects this general rule, but the cyclic one surprisingly shows an opposite variation of D with temperature above the ODT. This phenomenon can traduce an impossibility of the cyclic copolymers to stretch their backbone due to their excess of entropic penalty. Consequently, one might also suspect that the interdigitation at the interface is more pronounced in the case of linear than that of cyclic block copolymer chains. These data/hypothesis have to be confirm on other cyclic copolymers with different volume fractions and molar weights, but one can emphasize here another singularity due to the cyclization.

III-3.: Remarkable Highly Ordered Structure. Figure 4 describes the variation of the scattered intensity using SAXS as a function of the azimutal angle 2θ for the first-order peak at $q = 0.028$ $Å^{-1}$ of linear PS_{290}-*b*-PI_{110} at room temperature. In addition, the inset of Figure 4 illustrates the scattering intensities focusing on this first-order peak. The observed profiles reveal clearly cylindrically ordered and oriented structure highlighted by the "powder pattern" than can be observed even for the third peak. This way, we can calculated an average distance between the peak maxima observed in Figure 4 and obtain a typical value for a hexagonal oriented morphology of $\Delta\theta = 60°$. Even if no particular conditions have been applied to help this organization and especially orientation (excepted the annealing process), these well-defined and low polydisperse block copolymers have been able to orient in situ during the film formation.

Conclusion

The morphological behaviors of cyclic diblock copolymers and its corresponding linear PS-*b*-PI diblock have been investigated. The most important results are summarized in Table 2. The architectural difference

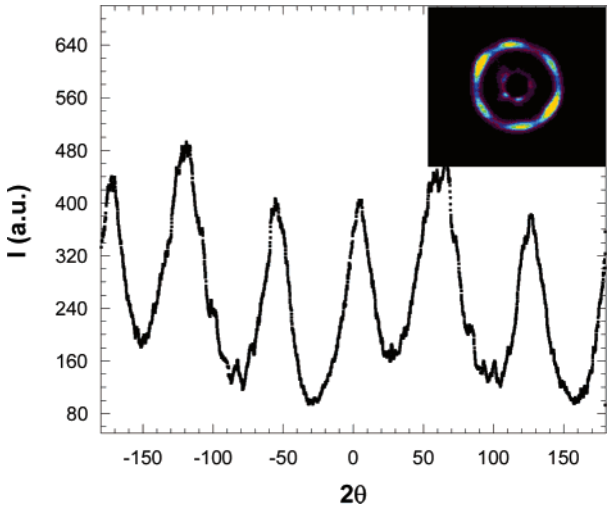

Figure 4. SAXS intensity distribution of the first-order peak as a function of the azimutal angle 2θ for linear PS_{290}-*b*-PI_{110} (the PI cylindrical domains are oriented parallel to the beam).

Scheme 2. Schematic Representation of the Cylindrical and Spherical Structures Obtained Respectively for Linear and Cyclic PS_{290}-*b*-PI_{110}[a]

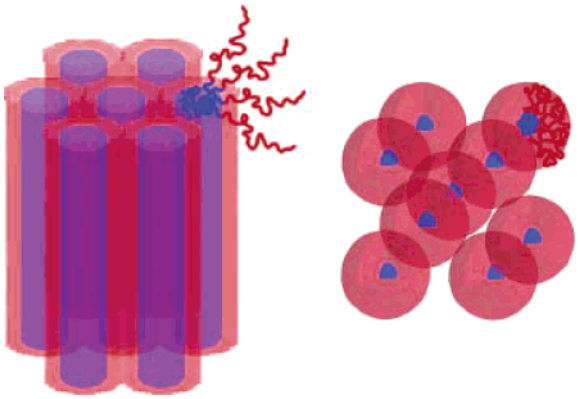

[a] The red color is for PS and the blue is for PI.

between a cyclic diblock copolymers and its corresponding linear leads to differences in their organized nanostructures as well as in their domain spacings. The cyclic morphology always has smaller domain spacing compared to its corresponding linear with a typical ratio of $\sqrt{2}$. In addition, the morphologies observed for linear and cyclic diblocks are quiet different: a highly ordered and even oriented structure for linear PS_{290}-*b*-PI_{110} and a poorly organized structure for cyclic PS_{290}-*b*-PI_{110}. A schematic representation of the resulting morphologies obtained for linear and cyclic copolymers (290 for PS and 110 for PI, corresponding to a volume fraction $\Phi_{PS} = 0.78$) is given in Scheme 2.

The results emphasized the difference between linear and cyclic block copolymers, not only in their domain size of organization, but also in the obtained morphology. More precisely, this paper investigated the effect of a "double constraint" in terms of loops in the poly-

styrene and polyisoprene domains of a cyclic diblock copolymer: a consistent change in the interfacial curvature of the system has been experimentally observed through a change from a cylindrical organization of the linear to a spherical-like morphology the cyclic diblock. Finally, to fully characterize the differences between these two chemical architectures, variable temperature SAXS allowed to determine the thermal stability of these ordered structures. ODT and critical $(\chi N)_{ODT}$ parameters have been calculated according to a mean field approach. The values obtained for cyclic were systematically lower than that for linear, confirming theoretical predictions for the linear block copolymer in one hand and a poor agreement with theoretical predictions for cyclic block copolymer chains. As far as the variation of domain spacing vs the temperature it had revealed that the interdigitation at the interface is more pronounced in the case of linear than that of cyclic block copolymer chains. By interdigitation, we mean an entanglement process that can fully take place (at the domain spacing interface) when dealing with linear chains (free end chains) but not with cyclic chains (no end chains). When comparing the domain spacings for linear and cyclicsystems in the ordered state, they are different ($D_{lin} > D_{cycl}$) mainly because of the size of the single molecule ($R_{g\ linear} = \sqrt{2} R_{g\ Cyclic}$). However, when increasing the temperature, D_{lin} decreases (free eneds chains lead to small domains; more easy to interdigitate) while D_{cycl} increases (no end chains lead to larger domains because of the topological constraints, less easy to interdigitate). This hypothesis certainly deserves more experimental evidence at different volume fractions. All the presented results demonstrate the need for more investigations (theoretically and experimentally) on the effect of architecture of the block on the organized structure made of block copolymer other than "classical" linear block copolymer chains.

Acknowledgment. R.B. acknowledges financial support from the CNRS, la "Région Aquitaine", and FEDER. ESRF beam time allocations (ID2 and BM2 (CRG-D2AM)) are gratefully acknowledged.

References and Notes

(1) Allen, C.; Maysinger, D.; Eisenberg, A. *Colloids Surf. B* **1999**, *16*, 3.
(2) Burke, S. E.; Shen, H.; Eisenberg, A. *Macromol. Symp.* **2001**, *175*, 273.
(3) Ciferri, A. *Supramolecular Polymers*; Marcel Dekker: New York, 2000.
(4) Hamley, I. W. *The Physics of Block Copolymers*; Oxford University Press: Oxford, England, 1998.
(5) Leibler, L. *Macromolecules* **1980**, *13*, 1602.
(6) (a) Bates, F. S. *Science* **1991**, *251*, 898. (b) Fredrickson, G. H.; Bates, F. S. *Annu. Rev. Mater. Sci.* **1996**, *26*, 501.
(7) (a) For some recent reviews, see, e.g.: (a) Klok, H.-A.; Lecommandoux, S. *Adv. Mater.* **2001**, *13*, 1217. (b) Lee, M.; Cho, B.-K.; Zin, W.-C. *Chem. Rev.* **2001**, *101*, 3869.
(8) (a) Benmouna, M.; Borsali, R.; Benoît, H *J. Phys. II (Paris)* **1993**, *3*, 1401. (b) Borsali, R.; Benmouna, M. *Europhys. Lett.* **1993**, *23*, 263. (d) Benmouna, M.; Borsali, R. *J. Polym. Sci., Part B: Phys. Ed.* **1994**, *32*, 981.
(9) Borsali, R.; Lecommandoux, S.; Pecora, R.; Benoît, H. *Macromolecules* **2001**, *34*, 4229.
(10) Marko, J. F. *Macromolecules* **1993**, *26*, 1442.
(11) (a) Yin, R.; Hogen-Esch, T. E. *Macromolecules* **1993**, *26*, 6952. (b) Yin, R.; Amis, J. E.; Hogen-Esch, T. E. *Macromol. Chem. Macromol. Symp.* **1994**, *85*, 217. (c) Lescanec, R. L.; Hadjuk, D. A.; Kim, G. Y.; Gan, Y. D.; Yin, R.; Gruner, S. M.; Hogen-Esch, T. E.; Thomas, E. L. *Macromolecules* **1995**, *28*, 3485.
(12) Iatrou, H.; Hadjichristidis, N.; Meier, G.; Frielinghaus, H.; Monkenbusch, M. *Macromolecules* **2002**, *35*, 5426.
(13) (a) Shappacher, M.; Deffieux, A. *Macromolecules* **2001**, *34*, 5827. (b) Shappacher, M.; Deffieux, A. *Macromol. Phys. Chem.* **2002**, *203*, 2463.
(14) He, T.; Zheng, G.-H.; Pan, C.-Y. *Macromolecules* **2003**, *36*, 5960.
(15) (a) Borsali, R.; Schappacher, M.; de Souza Lima, M.; Deffieux, A.; Lindner, P. *Polym. Prepr.* **2002**, *43(1)*, 201; (b) Borsali, R.; Schappacher, M.; et al. Manuscript in preparation.
(16) (a) Borsali, R.; Minatti, E.; Putaux, J.-L.; Schappacher, M.; Deffieux, A.; Viville, P.; Lazzaroni, R.; Narayanan, T. *Langmuir* **2002**, *19*, 6−9. (b) Minatti, E.; Viville, P.; Borsali, R.; Schappacher, M.; Deffieux, A.; Lazzaroni, R. *Macromolecules* **2003**, *36*, 4125−4133; (c) Minatti, E.; Borsali, R.; Schappacher, M.; Deffieux, A.; Narayanan, T.; Putaux, J.-L. *Macromol. Rapid Commun.* **2002**, *23*, 978−982. (d) Putaux, J.-L.; Minatti, E.; Borsali, R.; Schappacher, M.; Deffieux, A. *Macromolecules*, submitted for publication.
(17) Zhu, Y.; Gido, S. P.; Iatrou, H.; Hadjichristidis, N.; Mays, J. W. *Macromolecules* **2003**, *36*, 148.
(18) Takano, A.; Kadoi, O.; Hirahara, K.; Kawahara, S.; Isono, Y.; Suzuki, J.; Matsushita, Y *Macromolecules* **2003**, *36*, 3045.
(19) Mori, K.; Hasegawa, H.; Hashimoto, T. *Polymer* **1990**, *31*, 2368.
(20) Lai, C.; Russel, W. B.; Register, R. A. *Macromolecules* **2002**, *35*, 841−849.
(21) Schwab, M.; Stühn, B. *Phys. Rev. Lett.* **1996**, *76*, 924.
(22) (a) Adams, J. L.; Graessley, W. W.; Register, R. A. *Macromolecules* **1994**, *27*, 6026. (b) Han, C. D.; Baek, D. M.; Kim, J. K.; Ogawa, T.; Sakamoto, N.; Hashimoto, T. *Macromolecules* **1995**, *28*, 5043. (c) Sakamoto, N.; Hashimoto, T.; Han, C. D.; Kim, D.; Vaidya, N. Y. *Macromolecules* **1997**, *30*, 1621.
(23) Rosedal, J. H.; Bates, F. S.; Almdal, K.; Mortensen, K.; Wignall, G. D. *Macromolecules* **1995**, *28*, 1429.

MA035627R